Identification of potential anti-Alzheimer agents from *Pistacia atlantica* Desf. galls using UPLC fingerprinting, chemometrics, and molecular docking analyses

Ziyad Ben Ahmed[1,2], Fatiha Hefied[1], Toufik Hadj Mahammed[1], Veronique Seidel[3], Mohamed Yousfi[1]

[1]Laboratoire des Sciences Fondamentale, Université Amar Telidji, Laghouat, Algérie

[2]Department of Analytical Chemistry, Applied Chemometrics and Molecular Modelling, Vrije Universiteit Brussel (VUB), Brussels, Belgium

[3]Natural Products Research Laboratory, Strathclyde Institute of Pharmacy and Biomedical Sciences, University of Strathclyde, Glasgow, UK.

Abstract

The purpose of this study was to test extracts from *P. atlantica* Desf. galls (PAG) for anti-acetylcholinesterase (AChE) and anti-butyrylcholinesterase (BuChE) activity, and investigate the influence of harvesting time, plant gender, and growing location on such activity. The IC_{50} values of PAG extracts ranged from 56.42-68.94 µg/mL and 82.43-95.81µg/mL, respectively. Our findings revealed that the anti-AChE/BuChE activity of PAG extracts was relatively more influenced by the time of harvest than by plant gender and growing location. A combination of UPLC fingerprinting and chemometrics using partial least squares regression analysis identified the presence of two phenolic compounds, namely methyl gallate and digalloylquinic, as responsible for the anti-AChE/BuChE activity of PAG extracts. A molecular docking study further confirmed that both compounds were able to bind to AChE and BuChE and interact with key residues of the active sites of these enzymes.

Keywords: *Pistacia atlantica* galls, acetylcholinesterase, butyrylcholinesterase, chromatographic fingerprinting, molecular docking.

This is a peer-reviewed, accepted author manuscript of the following article: Ben Ahmed, Z., Hefied, F., Mahammed, T. H., Seidel, V., & Yousfi, M. (2022). Identification of potential anti-Alzheimer agents from Pistacia atlantica Desf. galls using UPLC fingerprinting, chemometrics, and molecular docking analyses. Journal of Food Processing and Preservation, [e16916]. https://doi.org/10.1111/jfpp.16916

Practical Applications

Pistacia atlantica Desf. is an important medicinal plant whose galls are traditionally used in many Mediterranean countries for the treatment of Alzheimer's disease. The combination of fingerprint technology with chemometrical approaches in this study enabled the putative identification of metabolites in *P. atlantica* gall extracts responsible for anticholinesterase activity. This investigation highlights the potential of *P. atlantica* galls as a promising source for the discovery and development of new anti-Alzheimer agents.

Correspondence

Ben Ahmed Ziyad

Université Amar Telidji, BP37G Laghouat, Algérie

Tel: +213 664413901, Fax: + 213 29 41 54 33

E-mail address: z.benahmed@lagh-univ.dz or Ziyad.Ben.Ahmed@vub.be

1. Introduction

Alzheimer's disease (AD), the most common form of dementia, is a progressive neurological disorder associated with a selective loss of cholinergic neurons, accumulation of amyloid-beta (Aβ) plaques and neurofibrillary tangles in the brain. The symptoms of AD include memory deterioration and a progressive impairment of cognitive functions. In 2020, it was estimated that almost 50 million people suffered from AD worldwide. The prevalence of AD is expected to triple by 2050 as the ageing population increases (Agatonovic-Kustrin et al., 2018; Le-Nhat-Thuy et al., 2020; Mumtaz et al., 2019). Increasing levels of the neurotransmitter acetylcholine (ACh) in the brain has been identified as a strategy to alleviate the cognitive and behavioral symptoms of AD (Ragab et al., 2019). The enzymes acetylcholinesterase (AChE) and butyrylcholinesterase (BuChE) are two structurally-related esterases/lipases of the α/β-hydrolases superfamily that are present in the nervous system (Cygler et al., 1993; Novichkova et al., 2019). The role of AChE in the brain is to degrade ACh into choline and acetic acid at the synaptic gaps of cholinergic neurons. There is also evidence that this enzyme promotes the formation of Aβ aggregates in AD (Alvarez et al., 1997; Ibrar et al., 2018).

Butyrylcholinesterase (BuChE) is a non-specific choline esterase that also plays an important role in AD, particularly in the late stage of the disease where its levels increase to compensate for a natural decline in AChE (Hartmann et al., 2007; Mushtaq et al., 2014;). Besides AD, BuChE has been implicated in various other diseases such as diabetes, obesity, and liver disorders (Zhao et al., 2021). Acetylcholinesterase inhibitors, such as donepezil, galantamine, and rivastigmine, are the only compounds to date that have proven effective in alleviating the symptoms of AD (Noori et al., 2021; Marucci et al., 2021). However, these drugs are expensive, and their long term use leads to various adverse side effects (Kundu and Dubey, 2021). There is a pressing need to discover novel, safer, cholinesterase inhibitors (ChEI) targeting AChE,

BuChE, or even both enzymes. Interest in the search for new potential ChEI from natural sources has been increasing over the past decades and various natural products have been reported worldwide for their anti-Alzheimer potential through targeting such enzymes (Hafez Ghoran and Kijjoa, 2021; Lai Shi Min et al., 2022; Murray et al., 2013).

Pistacia atlantica Desf. (Anacardiaceae), popularly known as "Butom", is one of four species within the genus *Pistacia* found in Algeria. It is a dioecious tree commonly growing in arid and semi-arid areas, including the Sahara Desert. The plant is used as functional food and different parts are employed in traditional medicine. Several phytochemicals, including phenolics, fatty acids, phytosterols, terpenoids, and volatile compounds, have been reported in this species. Crude extracts and isolated compounds from *P. atlantica* have demonstrated a wide range of pharmacological effects, including antioxidant, antimicrobial, anti-inflammatory, antinociceptive, wound healing, anticancer, antidiabetic, hepatoprotective antiparasitic, anti-urease, antihypertensive and interestingly anticholinesterase activity (Ben Ahmed et al., 2021). The essential oil from *P. atlantica* leaf and flower has previously displayed anti-AChE and anti-BuChE activity in vitro (Labed-Zouad et al., 2013). Similar results have been obtained with *P. atlantica* leaf and stem extracts (Achili et al., 2020; Peksel et al., 2010). The purpose of this study was to investigate the influence of plant gender, seasonality, and location of harvest on the anti-AChE and anti-BuChE activity of extracts prepared from *P. atlantica* Desf. galls (PAG). A combination of UPLC fingerprinting and chemometrics analysis using partial least squares (PLS) regression was employed to identify the peaks in the LC-chromatograms corresponding to the potential anti-AChE and anti-BuChE metabolites within PAG extracts. In addition, we explored, through molecular docking analysis, the ability of the identified metabolites to bind to each cholinesterase.

2. Materials and methods

2.1. Plant material

The identity of the gall samples was confirmed by S. Belhadj (Department of Agropastoralism, Faculty of Science, Achour Zian University, Djelfa, Algeria), and a voucher specimen (GL032010ULDB) was deposited in the herbarium of the Department of Biology, Faculty of Science, University of Laghouat (Algeria).

Galls from male (n = 5) and female (n = 5) *P. atlantica* Desf trees were collected periodically in the middle of each month, starting in July and ending November 2010. Trees with a similar age were sampled from Laghouat, located 400 km south of Algiers, Algeria. Laghouat (latitude 33°47'N; longitude 02°52'E; altitude 750 m) is characterized by an annual precipitation of 18 mm, an average summer temperature of 41.4 °C and clay soil type. Galls of one gender (collected from five randomly selected trees) were carefully mixed, dried and cleaned to remove insects and eggs, and then crushed manually, before storing them in polyethylene bags at ambient temperature in the dark until further use.

2.2. Preparation of extracts

The crude extract of *P. atlantica* galls (PAG) was prepared according to the method described by Hefied et al, (2020). Briefly, *P. atlantica* galls powder (2 g) was macerated in 40 mL methanol in the dark for 48 h at room temperature. The crude extract was filtered and the residue re-extracted with 30 mL of the same solvent for 24 h, and filtered again. The filtrates were combined and the methanol was removed using a rotary evaporator at 45°C. The final residue was dried, redissolved in methanol and kept at 6 °C until further analysis.

2.3. In vitro anti-AChE and anti-BuChE activity of PAG

The inhibitory effect of PAG on AChE and BuChE was studied using the Ellman colorimetric test (Cakmak and Gülçin, 2019). Stock solutions of PAG extracts (50 mg/mL) were prepared in methanol and serially-diluted to afford concentrations of 5, 25, 40, 60, 80 and 90 µg/mL. 100 µL of each extract dilution was transferred into a separate test tube with 150 µL of 100 mM sodium phosphate buffer (pH 8.0) and either 50 µL of AChE (5.32×10^{-3} U) or BuChE (6.85

$\times 10^{-3}$ U). The reaction mixtures were incubated at 25 °C for 15 min. Then, 5.50-dithio-bis(2-nitrobenzoic) acid (DTNB) (0.5 mM,10 µL), and either of acetylthiocholine iodide (0.71 mM, 50 µL) or butyrylthiocholine chloride (0.2 mM,10 µL) were added. The formation of 5-thio-2-nitrobenzoate, resulting from the reaction of DTNB with thiocholine released by the enzymatic hydrolysis of acetylthiocholine iodide or butyrylthiocholine chloride, respectively, was monitored at □□= 412 nm using a Shimadzu UV 160A spectrophotometer (Shimadzu, Kyoto, Japan). The anti-AChE and anti-BuChE activity was calculated as follows:

$$\text{Inhibition (\%)} = \frac{A_{cont}-(A_{sample}-A_{blank})}{A_{cont}} \times 100 \quad \textbf{(1)}$$

where A_{sample}, A_{blank}, and A_{cont} represents the absorbance of the sample, the blank (methanol instead of the enzyme solution), and the control (methanol instead of sample extract), respectively. The results were expressed as half-maximal inhibitory concentration (IC_{50}) values estimated by simple linear regression using OriginPro 8.6 (OriginLab, Northampton, MA, USA)

2.4. UPLC conditions

The method used for ultra-performance liquid chromatography (UPLC) fingerprinting was based on a previously published methodology with a mobile phase consisting of formic acid 0.1% (A) and methanol (B) with the following gradient: 0 min, 15% (B); 5 min, 30% (B); 10 min, 40% (B); 14 min, 45% (B); 16 min, 45% (B); 20 min, 55% (B); 25 min, 100% (B). The detection was performed at 254 nm (Hefny et al., 2018). Sample solutions were freshly prepared in methanol before injection (injection volume 2 µL) and filtered through a 0.22 µm cellulose regenerated membrane filter. Data was processed using Waters Empower™ software.

2.4. Partial Least Squares (PLS) regression analysis

2.4.1. Data preprocessing

Different data preprocessing approaches were applied, including column centering (CC), normalization, standard normal variate (SNV) and alignment of the data (Tistaert et al., 2012),

to minimize any sources of peak misalignment, baseline drift, and variation in sampling that could affect the chromatographic signals. Correlation optimized warping (COW) was applied to align corresponding peaks (i.e. correct for retention time shifts in chromatograms that may have originated from variations in flow rate, temperature and column aging) (Klein-Júnior et al., 2016; Tistaert et al., 2011)

2.4.2. Modelling

The Partial Least Squares (PLS) algorithm was used as a linear multivariate calibration technique to study the relationship between the $\boldsymbol{n} \times \boldsymbol{p}$ data matrix **X** (here, the LC-fingerprints) consisting of the samples (rows; $\boldsymbol{n} = 20$) and the time points (columns; $\boldsymbol{p} = 11501$) and an $n \times 1$ response vector y (here, anti-AChE and anti-BuChE activity). Regression coefficients were plotted as a function of time for each model (Ben Ahmed et al., 2018). Negative regression coefficients provided information on the metabolites potentially responsible for the anti-AChE and/ or anti-BuChE activity of PAG extracts. The optimal model complexity for each anti-ChE model was selected by determining the leave-one-out cross-validation with combination of low the root mean square error of cross-validation (RMSECV) value (Tables S1).

2.4.3. Validation

The leave-one-out cross-validation (CV) method (LOO-CV) was applied to calibrate the PLS model built with an optimal number of latent variables (LVs) based on the minimum value of the root mean-square error of cross-validation (RMSECV) (Ben Ahmed., 2020; Deng et al., 2015; Goodarzi et al., 2015; Li et al., 2021)

2.5. Molecular docking study

The crystal structures of acetylcholinesterase (PDB ID: 6G1U) and butyrylcholinesterase (PDB ID: 5LKR) were downloaded from the Protein Data Bank (http://www.rcsb.org/pdb). The secondary metabolites detected in the UPLC-MS analysis were used as the ligands for the docking study. The three-dimensional structure of each ligand was retrieved from the PubChem

database (http://pubchem.ncbi.nlm.nih.gov) using UCSF Chimera v1.15 (Pettersen et al., 2004). Before docking, the crystal structures of both proteins were processed using Discovery Studio v20.1, starting with the removal of all water molecules and heteroatoms to uncover the active site of each protein (Gilson and Zhou, 2007; Munawaroh et al., 2020). After that, polar hydrogens and Gasteiger charges were assigned with AutoDockTools (ADT) v1.5.6. The docking simulation and calculations were carried out using AutoDock Vina v1.2.3 (Trott and Olson, 2010). The exhaustiveness value was set to 24. The default grid box size was determined following a previously published protocol (Eberhardt et al ., 2021). The web server PrankWeb (https://prankweb.cz/) was used to predicte the active site of each protein (Jendele et al., 2019). The grid box for each target was established by enclosing the active site residues inside the box, with a grid spacing of 1 Å. The grid box parameters for AChE were centered on x = 3.777, y = −2.109, z = 21.658, with the size dimensions as 28 × 30 × 27. The grid box parameters for BuChE were centered on x = −19.964, y = 11.107, z = −41.291, with the size dimensions as 24 × 26 × 26. The protein targets were regarded as rigid while all ligand single bonds could rotate freely. The best ligand-receptor docked structure was selected based on the lowest docking score in kcal/mol (i.e. strongest binding affinity for the target enzyme). Intermolecular interactions between the docked ligands best poses and specific residues on the protein targets were visualized using PyMOL v1.7.4.5 (Schrödinger, LLC, New York, NY, USA) and LigPlot+ v2.2.4 (Salahuddin et al., 2020).

2.6. Statistical analysis

All experiments were carried out in triplicate and data were expressed as means ± SD. One-way analyses of variance (ANOVA) followed by Duncan *post hoc* tests were used to estimate the significance of the harvest month and plant gender on the anti-AChE and anti-BuChE activities. Paired *t*-tests were used to compare the differences in the averages of anti-AChE and anti-BuChE activities between harvest months, plant genders, and growing locations (Ben

Ahmed et al., 2017). Calculations were performed using SPSS v16 (SPSS, Prentice Hall, Chicago IL, USA, 2007). All chemometrics methods (i.e. column centering, normalizing, SNV, and PLS) applied to the data were performed using m-files, written in Matlab v7.1 (The MathWorks, Natick, MA, USA).

3. Results and discussion

3.1. Effect of harvesting time, plant gender, and growing location on the anti-AChE/BuChE activity of PAG extracts

PAG extracts from Laghouat demonstrated higher anti-ChE activity than those from Ain Oussera across the harvesting period (IC_{50} values from 56.42-66.38 µg/mL and 61.33-68.94 µg/mL, respectively for the anti-AChE activity; IC_{50} values from 82.43-95.81 µg/mL and 90.10-94.24 µg/mL, respectively for the anti-BuChE activity). A first one-way ANOVA revealed significant differences in anti-AChE activity at different harvesting periods for each combination of location and plant gender (p = 0.006, 0.026, 0.041 and 0.027 for GML, GFL, GMA and GFA, respectively). This was confirmed by Duncan *post-hoc* tests (Table 1). Thus, GML samples collected in October and August were significantly different in activity from those collected in the remaining months. GFL samples collected in August and September were significantly different in activity from each other. GFL samples collected in August were also significantly different from those collected in July and November. GFL samples collected in September were also significantly different from those collected in October. GML and GFL showed a similar pattern of seasonal fluctuations in their anti-AChE activity, with samples harvested in August and September associated with a maximal and minimal anti-AChE activity, respectively. Significance differences in activity were also observed when analyzing either GMA or GFA samples across the harvesting period, but GMA and GFA showed a similar pattern of seasonal fluctuations in their activity, with samples harvested in October and July associated with maximal and minimal anti-AChE activity, respectively.

[Table 1]

The paired-*t*-test carried out to evaluate the significance of gender differences on the anti-AChE activity of samples from different locations showed a statistical difference between galls collected from male/female plants growing in Laghouat ($p < 0.001$) but no statistical difference for samples from male/female plants growing in Ain Oussera ($p = 0.832$). This indicated that the anti-AChE activity of samples from Laghouat differed depending on the plant gender, and therefore the data obtained from male/female galls collected in Ain Oussera were combined. Another one-way ANOVA further showed no significant differences in the anti-AChE activity of samples growing in Ain Oussera during the harvesting period ($p > 0.05$). A paired *t*-test further revealed no significant difference in anti-AChE activity between samples from Ain Oussera and samples from Laghouat ($p > 0.05$). The anti-AChE activity of samples varied in a similar manner in both locations (Table 1).

A first one-way ANOVA to investigate differences within each location established that the anti-BuChE activity of samples from Laghouat varied significantly during the harvesting period ($p = 0.013$ and 0.002 for GML and GFL, respectively). This difference was not statistically significant for samples from Ain Oussera ($p = 0.634$ and 0.914 for GMA and GFA, respectively). Duncan post-hoc tests established that GML samples collected in August and October showed a significant difference in anti-BuChE activity from those collected in the remaining months. Significance differences in activity were also observed when analyzing GFL samples across the harvesting period. Maximal and minimal anti-BuChE activity was observed for samples collected in October (GML) and July (GFL) (Table 2).

[Table 2]

The paired-*t*-test showed no significant difference in anti-BuChE activity between male and female galls collected from Laghouat and Ain Oussera ($p = 0.071$ and 0.319, respectively). This suggests that plant gender did not have a significant effect on the anti-BuChE activity of

samples within each location and therefore results from both genders were combined into a single group within each location. Another one-way ANOVA revealed significant differences in the anti-BuChE activity of samples from Laghouat (p = 0.001), but not Ain Oussera (p = 0.0842), during the harvesting period. A paired-t-test further revealed that the anti-BuChE activity did not differ significantly between growing locations (p = 0.071). The anti-BuChE activity of samples varied in a similar manner in both locations (Table 2).

Overall, PAG extracts from male and female plants growing in both locations revealed better inhibitory activity on AChE than on BuChE (Figs.1 and 2).

[Figs.1 and 2]

Studies have revealed that extracts prepared from the same plant species but collected at different times of the year and/or different locations can present significant differences in their chemical profiles, which in turn affects biological activity (Shi et al, 20022; Bibi et al., 2022; Reyes-Vaquero et al., 2021). The effect of seasonal and plant gender variations on the essential oil composition of *P. atlantica* Desf. leaves and on the antioxidant activity of PAG have already been highlighted (Ben Ahmed et al., 2022; Gourine et al., 2010). The production/accumulation of metabolites in plants is also influenced by environmental biotic factors such as plant interactions with pathogens/insects/herbivores (Erb and Kliebenstein, 2020). *P. atlantica* galls are formed following attacks from insects, particularly aphids and chalcid wasps (Ben Ahmed et al., 2022). Therefore, it is reasonable to hyptothesize that the observed anti-ChE activity of PAG extracts could be due to the presence of defensive compounds targeting these enzymes in insects (Ryan and Byrne, 1988). To the best of our knowledge, the present study is the first to report on the anti-ChE activity of PAG extracts, including information on the best harvesting period to maximize the anti-ChE potential. Moreover, the galls were collected from *P. atlantica* growing in natural conditions, so it is difficult to determine which environmental factor is mainly responsible for observed variations because the changes are small and irregular(Tables

1 and 2). Therefore, seasonal variation of anti-ChE activity should be analysed over several years in order to confirm that October is the most useful harvest for anti-ChE activity compared to other harvest months. In this context, further studies with isolated constituents must be performed to determine how the anti-ChE compounds vary according to seasonality.

3.2. Identification of potential anti-AChE and/or anti-BuChE metabolites in PAG extracts using UPLC fingerprinting and chemometrics

The ultra-performance liquid chromatography (UPLC) fingerprints obtained for the 20 PAG samples analysed were preprocessed (Fig. 3) before being used to build the anti-AChE/anti-BuChE activity models used in PLS regression analysis. The peaks labelled as **2**, **3** and **4,** eluting at 3.12, 3.39, and 8.61 min, respectively, displayed negative regression coefficients in the anti-AChE activity model, suggesting their potential as anti-AChE metabolites. In addition, the model showed two major positive peaks (i.e. unlikely to contribute to the anti-AChE activity) labelled as **1** and **5** and eluting at 1.16 and 9.2 min, respectively (Fig. 4). The peaks labelled as **2**, **3** and **5,** eluting at 3.12, 3.39, and 9.20 min respectively, displayed negative regression coefficients in the anti-BuChE activity model suggesting their potential as anti-BuChE metabolites. In addition, the model showed two peaks with positive regression coefficients (i.e. unlikely to contribute to the anti-BuChE activity) labelled as **1** and **4** and eluting at 1.16 and 8.61 min, respectively (Fig. 5). From these results, it could be summarized that peak **4** and **5** were linked to a selective anti-AChE and anti-BuChE effect, respectively, whilst peak **2** and **3** showed dual anti-AChE and anti-BuChE properties.

[Figs.4 and 5]

As the complexity of herbal extracts often makes it often difficult to purify bioactive compounds within a reasonable time limit, the use of a combination of LC fingerprinting and chemometrics has gained in popularity in recent years as an efficient method to identify metabolites potentially responsible for a given biological activity (Ben Ahmed et al., 2022; Ertas et al., 2021).

Our findings demonstrated the applicability of LC fingerprinting linked to chemometrics to identify potential anti-ChE metabolites in PAG extracts. Peaks **1**, 2, **3**, **4**, and **5** were previously characterized as the phenolic compounds quinic acid, methyl gallate, digalloylquinic acid, methyl digallate, and valoneic acid dilactone, respectively. Previous reports have shown that bioactive phytochemicals, like phenolic compounds, could form complexes with enzymes, changing their biological structures and inhibiting their activity (Zhang et al., 2022). Another interesting observation is that (**1-5**) were previously predicted to be responsible for the antioxidant activity of PAG extracts (Ben Ahmed et al., 2022). It could be assumed that these phenolic compounds may also contribute in reducing oxidative stress associated with AD and other neurodegenerative disorders (Ten et al., 2018; Arruda et al., 2020).

3.3. Molecular interaction analysis

The binding affinity of methyl gallate and digalloylquinic acid in the active site of AChE and BuChE was further predicted using a molecular docking approach. Methyl gallate and digalloylquinic acid displayed docking scores of −6.47 and −8.26 kcal/mol, respectively (Table 3). The active site of AChE is a long gorge with a length of approximately 20 Å. The bottom of the gorge contains several sub-sites. The peripheral anionic site (PAS) is located around the entrance of the active site gorge (approximately 18 Å away from the active site). The PAS region consists of several aromatic residues, including Asp72, Trp279, Tyr70, Tyr121, and Tyr334, and is considered to exert important functions related to both ACh hydrolysis and Aβ aggregation (Bartolini et al., 2003). The catalytic active site (CAS) is responsible for the hydrolysis of ACh through a catalytic triad consisting of Ser200, Glu327, and His440. The amino acids Phe288 and Phe290 form an acyl pocket, while Trp84 and Phe330 make up the anionic site. There is also an oxyanion hole that binds with the acetylcholine carbonyl oxygen, and which contains Gly118, Gly119, and Ala201 residues (Chen et al., 2017).

[Table 3]

The docking analysis revealed that the top ranked conformations of methyl gallate and digalloylquinic acid were well accommodated within the active site of AChE. Each ligand displayed different types of interactions with the active site residues of the target enzyme as shown in Fig. 6a and b. Methyl gallate showed interactions with the PAS region of AChE by interacting with Tyr121 through a hydrophobic interaction. It also formed a hydrophobic interaction with His440, a critical residue in the Ser200-Glu327-His440 catalytic triad of the CAS region of AChE. Such interactions suggest that methyl gallate could exert its anti-AChE activity by hindering the approach of acetylcholine to CAS. The carbonyl group at C7 in methyl gallate established one hydrogen bond with Ser 122 (3.13 Å). Methyl gallate also interacted via hydrophobic interactions with Trp84 and Phe330 residues of the anionic site of AChE, and showed two other hydrophobic interactions with Glu199 and Gly 441 (Fig. 6a).

Digalloylquinic acid established hydrogen bonds with Arg289, and Phe331, via its hydroxyl group in C5 (3.09/2.71 Å) and C1 (3.16 Å), respectively. It also interacted through a hydrogen bond via its carbonyl group at C8 (3.07 Å) with Tyr121 of the PAS region. Hydrophobic interactions between the docked conformation and the Tyr70, Trp279 and Tyr334 residues of PAS further stabilized this ligand within the PAS region. Digalloylquinic acid also showed hydrophobic interactions with Phe288 and Phe290 of the acyl binding pocket of AChE. Such interactions suggest a strong binding of this compound at the bottom of the pocket, potentially preventing the binding of acetylcholine. At the anionic site of AChE, digalloylquinic acid interacted with Phe330 through a hydrophobic interaction. Other residues, including Ile287, Gly335, as well as Ser286, were also implicated in the anchoring of this ligand via hydrophobic interactions (Fig.6b).

[Fig. 6]

The predicted binding affinity and interactions of methyl gallate and digalloylquinic acid with the active site residues of BuChE were also analyzed by molecular docking. Methyl gallate and

digalloylquinic acid had docking scores of −5.98 and −9.10 kcal/mol towards BuChE, respectively (Table 4). The active site of BuChE is comprised of the CAS site with three important residues (Ser198, His438, Glu325), a choline binding site or cation-π site (Trp82), an oxyanion hole (Gly116, Gly117, Ala199), an acyl binding site (hydrophobic pocket) (Leu286, Val288), and PAS (Asp70) (Ogidigo et al., 2021). The hydroxyl group in C5 of methyl gallate showed hydrogen bond interactions with Tyr128 and Glu197 (3.08 and 3.04 Å, respectively) while its hydroxyl group in C6 formed a hydrogen bond with Tyr128 (2.86 Å). Methyl gallate further interacted with the His438 residue of CAS via a hydrophobic interaction, and developed a π-cation interaction with the Trp82 residue of the cation-π site. The docked conformation was further stabilized by hydrophobic interactions with Tyr440, Gly115, and Ile442 (Fig. 7a). Digalloylquinic acid interacted via four hydrogen bonds with Glu197 (3.34 Å), Ala328 (3.14 Å) and Tyr128 (3.11 and 2.70 Å). Its hydroxyl group in C17 interacted with Glu197 and Tyr128, respectively, while its hydroxyl group groups in C5 and C20 interacted with Ala328 and Tyr128, respectively. It also established hydrophobic interactions with Gly115, Met437, Trp430, Phe329, Tyr332, Thr120 and Ile69. Digalloylquinic acid also interacted with the Gly116 residue of the oxyanion hole and the Asp70 residue of PAS via hydrophobic interactions. It further interacted with Trp82 in the cation-π site of BuChE (Fig.7b).

[Table 4]

Overall, methyl gallate interacted with residues present in multiple locations within the active site of AChE, including the PAS and CAS regions. Digalloylquinic acid interacted mainly with residues in the PAS region. As CAS is responsible for the hydrolysis of ACh and PAS is involved in both ACh hydrolysis and Aβ aggregation (Bartolini et al., 2003; Chen et al., 2017), these results suggest that both methyl gallate and digalloylquinic acid have the potential to influence the catalytic activity of AChE as well as its effect on Aβ plaque aggregation. Digalloylquinic acid also interacted with Trp82, along with Tyr128, Gly115, and Glu197 that

have been identified as important residues for an inhibitory effect on BuChE in line with previous studies (Chen et al., 2017, Iqbal et al., 2021). Digalloylquinic acid had a higher predictive binding affinity towards AChE/BuChE than methyl gallate and interacted with each enzyme via more hydrogen bonds and hydrophobic interactions compared to methyl gallate. Previous studies have indicated that the presence of multiple interactions (particularly via hydrogen bonds) between a ligand with a phenolic structure and the active site residues of AChE and BuChE supported potentially high inhibitory activity (Ali et al., 2016; Mansha et al., 2021).

[Fig. 7]

4. Conclusion

This study is the first to describe the effect of harvesting time, plant gender, and growing locations on the anti-AChE and anti-BuChE activity of PAG extracts. We observed that the anti-AChE/BuChE activity of PAG extracts was relatively more influenced by the time of harvest than by plant gender and growing location, with October identified overall as the best harvesting month for optimal activity. Overall, PAG extracts from Laghouat demonstrated higher anti-ChE activity than those from Ain Oussera across the harvesting period. Those prepared from male/female plants regardless of growing locations had better inhibitory activity on AChE than on BuChE. Combining data on the anti-ChE activity of PAG extracts with their UPLC fingerprints enabled us to construct a multivariate calibration model using PLS regression analysis, and calculate regression coefficients predicting the peaks in the LC-chromatograms corresponding to methyl gallate and digalloylquinic potentially responsible for both anti-AChE and anti-BuChE activity. Molecular docking analyses confirmed that methyl gallate interacted with key amino acids in the active site of AChE (CAS and PAS regions) and BuChE (CAS region), while digalloylquinic acid interacted with important residues in the active site of AChE and BuChE (PAS regions in both cases). Our findings suggest that *P.*

atlantica galls may serve as a potential source for the discovery and development of new anti-AChE/BuChE agents for the management of AD. Further in vitro and in vivo studies are warranted to screen the active phenolic compounds identified in our PAG extracts for anti-AChE/BuChE activity, as well as characterize any further active constituents that may be responsible for the observed anti-ChE activity.

Contributors ' statement

Concept and design of work: Yousfi M, Seidel V, Ben Ahmed Z; **Data collection**: Ben Ahmed Z; Hefied F, Hadj Mahammed T; **Statistical analysis**: Ben Ahmed Z; **Analysis and interpretation of data**: Ben Ahmed Z, Seidel V; **Drafting of manuscript**: Ben Ahmed Z, Seidel V; **Critical revision of manuscript**: Seidel V, Yousfi M.

Declaration of competing interest

The authors declare that they have no known competing financial interests or personal relationships that could have appeared to influence the work reported in this paper.

Acknowledgement

The authors thank the General Directorate of Research and Technology Development, Ministry of Higher Education and Scientific Research of Algeria (DGRSDT) for financial support.

References

Achili, I., Amrani, A., Bensouici, C., Gül, F., Altun, M., Demirtas, I., Benayache, S. (2020). Chemical constituents, antioxidant, anticholinesterase and antiproliferative effects of Algerian *Pistacia atlantica* Desf. extracts. *Recent Patents on Food, Nutrition & Agriculture*, *11(3)*, 249-256.

Agatonovic-Kustrin, S., Kettle, C., Morton, D. W. (2018). A molecular approach in drug development for Alzheimer's disease. *Biomedicine & Pharmacotherapy*, *106*, 553-565.

Ali, B., MS Jamal, Q., Shams, S., A Al-Wabel, N., U Siddiqui, M., A Alzohairy, M., A. Al Karaawi, M., Kumar Kesari, K., Mushtaq, G., A Kamal, M. (2016). In silico analysis of green tea polyphenols as inhibitors of AChE and BChE enzymes in Alzheimer's disease treatment. *CNS & Neurological Disorders-Drug*, *15*(5), 624-628.

Alvarez, A., Opazo, C., Alarcón, R., Garrido, J., Inestrosa, N. C. (1997). Acetylcholinesterase promotes the aggregation of amyloid-β-peptide fragments by forming a complex with the growing fibrils. *Journal of Molecular Biology*, *272*(3), 348-361.

Arruda, H. S., Neri-Numa, I. A., Kido, L. A., Júnior, M. R. M., Pastore, G. M. (2020). Recent advances and possibilities for the use of plant phenolic compounds to manage ageing-related diseases. *Journal of Functional Foods*, *75*, 104203.

Bartolini, M., Bertucci, C., Cavrini, V., Andrisano, V. (2003). β-Amyloid aggregation induced by human acetylcholinesterase: inhibition studies. *Biochemical Pharmacology*, *65*(3), 407-416.

Ben Ahmed, Z., Hefied, F., Yousfi, M., Demeyer, K., Vander Heyden, Y. (2022). Study of the antioxidant activity of *Pistacia atlantica* Desf. Gall extracts and evaluation of the responsible compounds. *Biochemical Systematics and Ecology*, *100*, 104358.

Ben Ahmed, Z., Mohamed, Y., Johan, V., Dejaegher, B., Demeyer, K., Vander Heyden, Y. (2020). Defining a standardized methodology for the determination of the antioxidant capacity: case study of *Pistacia atlantica* leaves. *Analyst*, *145(2)*, 557-571.

Ben Ahmed, Z., Yousfi, M., Viaene, J., Dejaegher, B., Demeyer, K., Mangelings, D., Vander Heyden, Y. (2017). Seasonal, gender and regional variations in total phenolic, flavonoid, and condensed tannins contents and in antioxidant properties from *Pistacia atlantica* ssp. leaves. *Pharmaceutical Biology*, *55(1)*, 1185-1194.

Ben Ahmed, Z., Yousfi, M., Viaene, J., Dejaegher, B., Demeyer, K., Vander Heyden, Y. (2021). Four *Pistacia atlantica* subspecies (*atlantica*, *cabulica*, *kurdica* and *mutica*): A review of their botany, ethnobotany, phytochemistry and pharmacology. *Journal of Ethnopharmacology*, *265*, 113329.

Ben Ahmed, Z., Yousfi, M., Viaene, J., Dejaegher, B., Demeyer, K., Mangelings, D., Vander Heyden, Y. (2018). Potentially antidiabetic and antihypertensive compounds identified from *Pistacia atlantica* leaf extracts by LC fingerprinting. *Journal of Pharmaceutical and Biomedical Analysis*, *149*, 547-556.

Bibi, N., Shah, M. H., Khan, N., Al-Hashimi, A., Elshikh, M. S., Iqbal, A., Ahmed, S., Abbasi, A. M. (2022). Variations in Total Phenolic, Total Flavonoid Contents, and Free Radicals' Scavenging Potential of Onion Varieties Planted under Diverse Environmental Conditions. *Plants (Basel)*, *11(7)*, 950.

Cakmak, K. C., Gülçin, İ. (2019). Anticholinergic and antioxidant activities of usnic acid-An activity-structure insight. *Toxicology Reports*, *6*, 1273-1280.

Chen, Y., Lin, H., Yang, H., Tan, R., Bian, Y., Fu, T., Li, W., Wu, L., Pei, Y., Sun, H. (2017). Discovery of new acetylcholinesterase and butyrylcholinesterase inhibitors through structure-based virtual screening. *RSC advances*, *7*(6), 3429-3438.

Cygler, M., Schrag, J. D., Sussman, J. L., Harel, M., Silman, I., Gentry, M. K., Doctor, B. P. (1993). Relationship between sequence conservation and three-dimensional structure in a large family of esterases, lipases, and related proteins. *Protein Science*, *2(3)*, 366-382.

Deng, B. C., Yun, Y. H., Liang, Y. Z., Cao, D. S., Xu, Q. S., Yi, L. Z., Huang, X. (2015). A new strategy to prevent over-fitting in partial least squares models based on model population analysis. *Analytica Chimica Acta*, *880*, 32-41.

Eberhardt, J., Santos-Martins, D., Tillack, A. F., Forli, S. (2021). AutoDock Vina 1.2. 0: New docking methods, expanded force field, and python bindings. *Journal of Chemical Information and Modeling*, *61*(8), 3891-3898.

Erb, M., Kliebenstein, D. J. (2020). Plant secondary metabolites as defenses, regulators, and primary metabolites: the blurred functional trichotomy. *Plant physiology*, *184*(1), 39-52.

Ertas, A., Firat, M., Yener, I., Akdeniz, M., Yigitkan, S., Bakir, D., Cakir, C., Yilmaz, M. A., Ozturk, M., Kolak, U. (2021). Phytochemical Fingerprints and Bioactivities of Ripe Disseminules (Fruit-Seeds) of Seventeen *Gundelia* (Kenger-Kereng Dikeni) Species from Anatolia with Chemometric Approach. *Chemistry & Biodiversity*, *18(8)*, e2100207.

Gilson, M. K., Zhou, H. X. (2007). Calculation of protein-ligand binding affinities. *Annual Review of Biophysics and Biomolecular Structure*, *36*, 21-42.

Goodarzi, M., Sharma, S., Ramon, H., & Saeys, W. (2015). Multivariate calibration of NIR spectroscopic sensors for continuous glucose monitoring. *TrAC Trends in Analytical Chemistry*, *67*, 147-158.

Gourine, N., Yousfi, M., Bombarda, I., Nadjemi, B., Gaydou, E. (2010). Seasonal variation of chemical composition and antioxidant activity of essential oil from *Pistacia atlantica* Desf. leaves. *Journal of the American Oil Chemists' Society*, *87*(2), 157-166.

Hafez Ghoran, S., Kijjoa, A. (2021). Marine-Derived Compounds with Anti-Alzheimer's Disease Activities. *Marine Drugs*, *19*(8), 410.

Hartmann, J., Kiewert, C., Duysen, E. G., Lockridge, O., Greig, N. H., Klein, J. (2007). Excessive hippocampal acetylcholine levels in acetylcholinesterase-deficient mice are moderated by butyrylcholinesterase activity. *Journal of Neurochemistry*, *100(5)*, 1421-1429.

Hefied, F., Ben Ahmed, Z., Yousfi, M. (2020). In vitro antioxidant and α-amylase inhibitory potential of methanolic and lipid fractions from *Pistacia atlantica* Desf. galls. *Journal of Food Processing and Preservation*, *44(12*), e14956.

Hefny Gad, M., Tuenter, E., El-Sawi, N., Younes, S., El-Ghadban, E. M., Demeyer, K., Mangelings, D. (2018). Identification of some bioactive metabolites in a fractionated methanol extract from *Ipomoea aquatica* (aerial parts) through TLC, HPLC, UPLC-ESI-QTOF-MS and LC-SPE-NMR fingerprints analyses. *Phytochemical Analysis*, *29(1)*, 5-15.

Ibrar, A., Khan, A., Ali, M., Sarwar, R., Mehsud, S., Farooq, U., Al-Harrasi, A. (2018). Combined in vitro and in silico studies for the anticholinesterase activity and pharmacokinetics of coumarinyl thiazoles and oxadiazoles. *Frontiers in Chemistry*, *6*, 61-73.

Iqbal, D., Rehman, M. T. (2021). Bin Dukhyil A., Rizvi SMD, Al Ajmi MF, Alshehri BM, Banawas S., Khan MS, Alturaiki W., Alsaweed M. High-Throughput Screening and Molecular Dynamics Simulation of Natural Product-like Compounds against Alzheimer's Disease through Multitarget Approach. *Pharmaceuticals*, *14*, 937.

Klein-Júnior, L. C., Viaene, J., Tuenter, E., Salton, J., Gasper, A. L., Apers, S., Vander Heyden, Y. (2016). The use of chemometrics to study multifunctional indole alkaloids from *Psychotria nemorosa* (*Palicourea comb*. nov.). Part II: Indication of peaks related to the inhibition of butyrylcholinesterase and monoamine oxidase-A. *Journal of Chromatography A*, *1463*, 71-80.

Kundu, D., Dubey, V. K. (2021). Potential alternatives to current cholinesterase inhibitors: an in silico drug repurposing approach. *Drug Development and Industrial Pharmacy*, *47(6)*, 919-930.

Lai Shi Min, S., Liew, S. Y., Chear, N. J. Y., Goh, B. H., Tan, W. N., Khaw, K. Y. (2022). Plant Terpenoids as the Promising Source of Cholinesterase Inhibitors for Anti-AD Therapy. *Biology*, *11(2)*, 307.

Le-Nhat-Thuy, G., Thi, N. N., Pham-The, H., Thi, T. A. D., Thi, H. N., Thi, T. H. N., Van Nguyen, T. (2020). Synthesis and biological evaluation of novel quinazoline-triazole hybrid compounds with potential use in Alzheimer's disease. *Bioorganic & Medicinal Chemistry Letters*, *30(18*), 127404.

Li, Z., Wang, X., Kruger, U. (2021). Efficient cross-validatory algorithm for identifying dynamic nonlinear process models. *Control Engineering Practice*, *111*, 104787.

Mansha, M., Taha, M., Ullah, N. (2021). The design of fluoroquinolone-based cholinesterase inhibitors: Synthesis, biological evaluation and in silico docking studies. *Arabian Journal of Chemistry*, *14*(7), 103211.

Marucci, G., Buccioni, M., Dal Ben, D., Lambertucci, C., Volpini, R., Amenta, F. (2021). Efficacy of acetylcholinesterase inhibitors in Alzheimer's disease. *Neuropharmacology*, *190*, 108352.

Mumtaz, A., Majeed, A., Zaib, S., Rahman, S. U., Hameed, S., Saeed, A., Iqbal, J. (2019). Investigation of potent inhibitors of cholinesterase based on thiourea and pyrazoline derivatives: Synthesis, inhibition assay and molecular modeling studies. *Bioorganic Chemistry*, *90*, 103036.

Munawaroh, H. S. H., Gumilar, G. G., Nurjanah, F., Yuliani, G., Aisyah, S., Kurnia, D., Show, P. L. (2020). In-vitro molecular docking analysis of microalgae extracted phycocyanin as an anti-diabetic candidate. *Biochemical Engineering Journal*, *161*, 107666.

Murray, A. P., Faraoni, M. B., Castro, M. J., Alza, N. P., Cavallaro, V. (2013). Natural AChE inhibitors from plants and their contribution to Alzheimer's disease therapy. *Current Neuropharmacology*, *11*(4), 388-413.

Mushtaq, G., H Greig, N., A Khan, J., A Kamal, M. (2014). Status of acetylcholinesterase and butyrylcholinesterase in Alzheimer's disease and type 2 diabetes mellitus. CNS & *Neurological Disorders-Drug Targets*, *13(8)*, 1432-1439.

Noori, T., Dehpour, A. R., Sureda, A., Sobarzo-Sanchez, E., Shirooie, S. (2021). Role of natural products for the treatment of Alzheimer's disease. *European Journal of Pharmacology*, *2021*, 173974.

Novichkova, D. A., Lushchekina, S. V., Dym, O., Masson, P., Silman, I., Sussman, J. L. (2019). The four-helix bundle in cholinesterase dimers: structural and energetic determinants of stability. *Chemico-Biological Interactions*, *309*, 108699.

Ogidigo, J. O., Anosike, C. A., Joshua, P. E., Ibeji, C. U., Ekpo, D. E., Nwanguma, B. C., Nwodo, O. F. C. (2021). UPLC-PDA-ESI-QTOF-MS/MS fingerprint of purified flavonoid enriched fraction of *Bryophyllum pinnatum*; antioxidant properties, anticholinesterase activity and in silico studies. *Pharmaceutical Biology*, *59*(1), 444-456.

Peksel, A., Arisan-Atac, I. N. C. I., Yanardag, R. (2010). Evaluation of antioxidant and antiacetylcholinesterase activities of the extracts of *Pistacia atlantica* Desf. Leaves. *Journal of Food Biochemistry*, 34(3), 451-476.

Pettersen, E. F., Goddard, T. D., Huang, C. C., Couch, G. S., Greenblatt, D. M., Meng, E. C., Ferrin, T. E. (2004). UCSF Chimera-a visualization system for exploratory research and analysis. *Journal of Computational Chemistry*, *25(13)*, 1605-1612.

Ragab, H. M., Teleb, M., Haidar, H. R., Gouda, N. (2019). Chlorinated tacrine analogs: Design, synthesis and biological evaluation of their anti-cholinesterase activity as potential treatment for Alzheimer’s disease. *Bioorganic Chemistry*, *86*, 557-568.

Reyes-Vaquero, L., Bueno, M., Ventura-Aguilar, R. I., Aguilar-Guadarrama, A. B., Robledo, N., Sepúlveda-Jiménez, G., EmilioVanegas-Espinoza, P., Ibáñez, I., Del Villar-Martínez, A.

A. (2021). Seasonal variation of chemical profile of *Ruta graveolens* extracts and biological activity against *Fusarium oxysporum*, *Fusarium proliferatum* and *Stemphylium vesicarium*. *Biochemical Systematics and Ecology, 95*, 104223.

Ryan, M. F., Byrne, O. (1988). Plant-insect coevolution and inhibition of acetylcholinesterase. *Journal of Chemical Ecology*, *14*(10), 1965-1975.

Salahuddin, M. A. H., Ismail, A., Kassim, N. K., Hamid, M., Ali, M. S. M. (2020). Phenolic profiling and evaluation of in vitro antioxidant, α-glucosidase and α-amylase inhibitory activities of *Lepisanthes fruticosa* (Roxb) Leenh fruit extracts. *Food Chemistry*, *331*, 127240.

Shi, Y., Yang, L., Yu, M., Li, Z., Ke, Z., Qian, X., Ruan, X., He, L., Wei, F., Zaho, Y, Wang, Q. (2022). Seasonal variation influences flavonoid biosynthesis path and content, and antioxidant activity of metabolites in *Tetrastigma hemsleyanum* Diels & Gilg. *Plos one*, *17*(4), e0265954.

Tan, B. L., Norhaizan, M. E., Liew, W. P. P., Sulaiman Rahman, H. (2018). Antioxidant and oxidative stress: a mutual interplay in age-related diseases. *Frontiers in pharmacology*, *9*, 1162.

Tistaert, C., Chataigné, G., Dejaegher, B., Rivière, C., Hoai, N. N., Van, M. C., Vander Heyden, Y. (2012). Multivariate data analysis to evaluate the fingerprint peaks responsible for the cytotoxic activity of *Mallotus* species. *Journal of Chromatography B*, *910*, 103-113.

Tistaert, C., Dejaegher, B., Vander Heyden, Y. (2011). Chromatographic separation techniques and data handling methods for herbal fingerprints: a review. *Analytica Chimica Acta*, *690*(2), 148-161.

Trott, O., Olson, A. J. (2010). AutoDock Vina: improving the speed and accuracy of docking with a new scoring function, efficient optimization, and multithreading. *Journal of Computational Chemistry*, *31*(2), 455-461.

Zhang, Y., Cai, P., Cheng, G., Zhang, Y. (2022). A Brief Review of Phenolic Compounds Identified from Plants: Their Extraction, Analysis, and Biological Activity. *Natural Product Communications*, *17*(1), 1934578X211069721.

Zhao, S., Xu, J., Zhang, S., Han, M., Wu, Y., Li, Y., Hu, L. (2021). Multivalent butyrylcholinesterase inhibitor discovered by exploiting dynamic combinatorial chemistry. *Bioorganic Chemistry*, *108*, 104656.

Caption Figures

Fig.1. Anti-AChE activity (expressed as % inhibition) of various concentrations of gall extracts of *P. atlantica* male and female plants collected in Laghouat (a) and Ain Oussera (b) (GML-GFL): male (ML) and female (FL) gall collected in Laghouat, (GMA-GFA): male (MA) and female (FA) galls collected in Ain Oussera.

Fig. 2. Anti-BuChE activity (expressed as % inhibition) of various concentrations of gall extracts of *P. atlantica* male and female plants collected in Laghouat (a) and Ain Oussera (b) (GML-GFL): male (ML) and female (FL) gall collected in Laghouat, (GMA-GFA): male (MA) and female (FA) galls collected in Ain Oussera.

Fig. 3. Warped chromatograms of the 20 PAG samples, acquired on an Acquity BEH C18 UPLC column with a mobile phase consisting of formic acid 0.1% (A) and methanol (B), a column temperature of 25 °C, a flow rate of 0.3 mL/min, injection volume of 2 µL, and detection wavelength at 254 nm (see Materials and methods section for reference).

Fig. 4. (a) UPLC chromatograms and (b) PLS regression coefficients after column centering of the 20 PAG samples analyzed in the anti-AChE activity model.

Fig.5. (a) UPLC chromatograms and (b) PLS regression coefficients after normalization and column centering of the 20 PAG samples analyzed in the anti-BuChE activity model.

Fig. 6. Molecular docking analysis showing the interactions of methyl gallate (a) and digalloylquinic acid (b) with the binding site of AChE.

Fig. 7. Molecular docking analysis showing the interactions of methyl gallate (a) and digalloylquinic acid (b) with the binding site of BuChE.

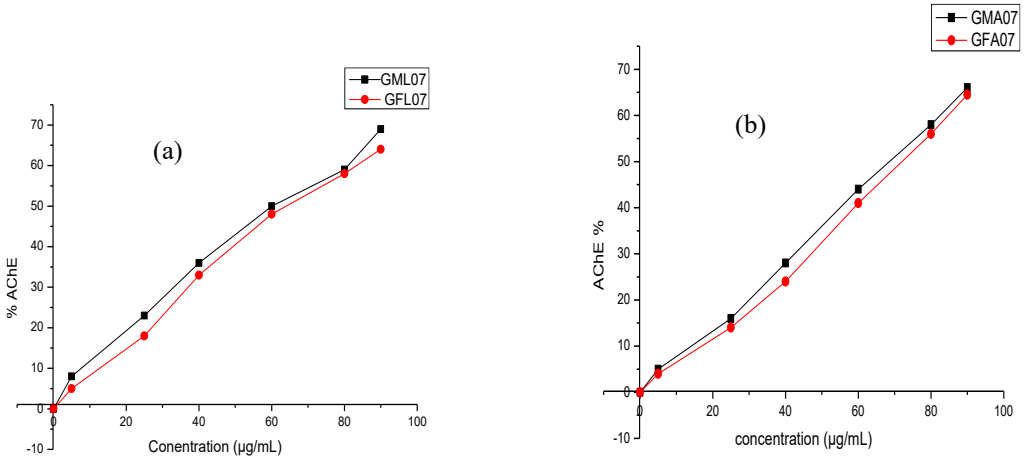
(a)
GML07
GFL07
% AChE
Conentration (µg/mL)
(b)
GMA07
GFA07
AChE %
concentration (µg/mL)

Fig.1

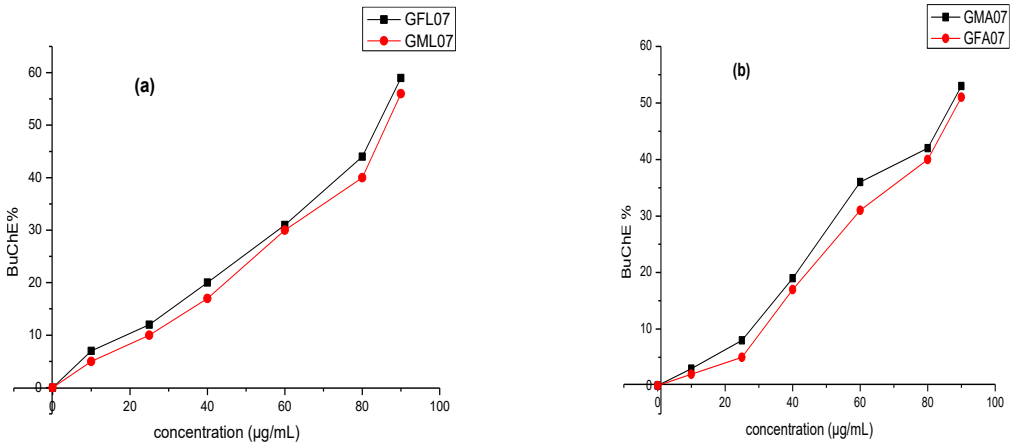
GFL07
GML07
(a)
BuChE%
concentration (µg/mL)
GMA07
GFA07
(b)
BuChE %
concentration (µg/mL)

Fig.2

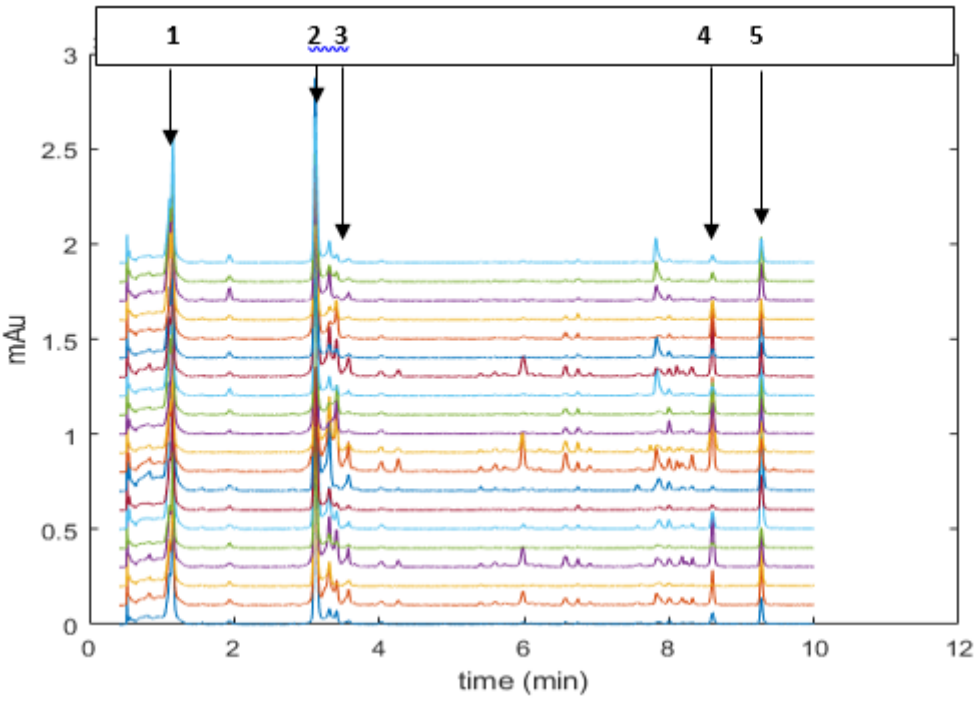

Fig.3

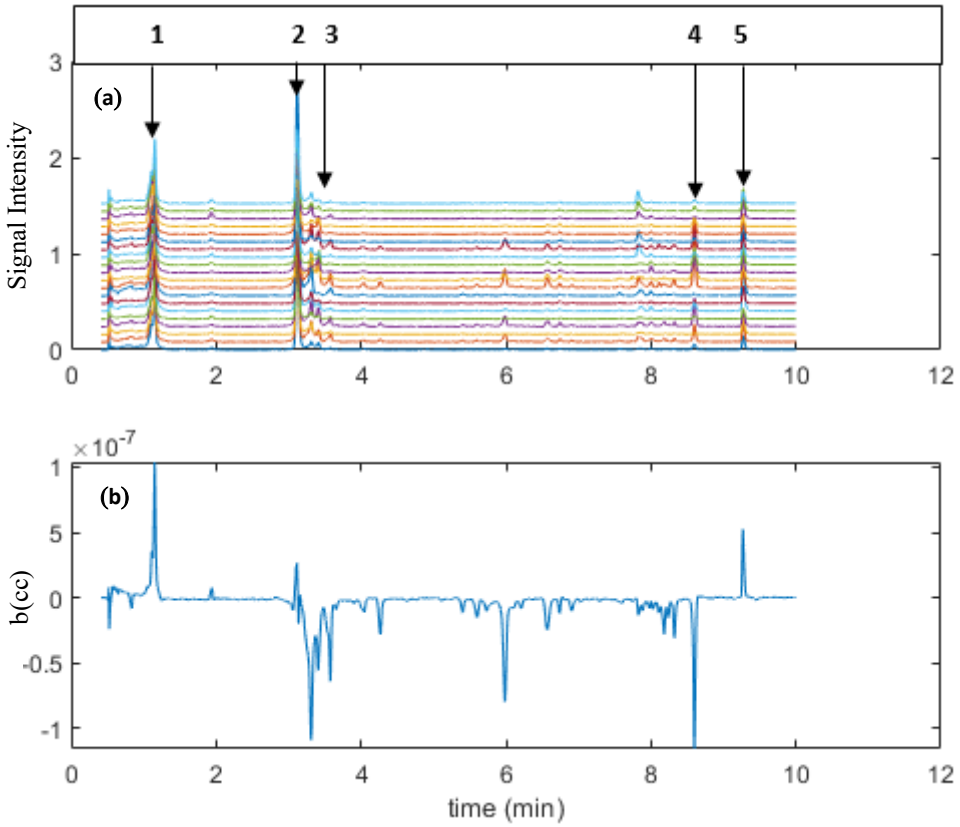

Fig.4

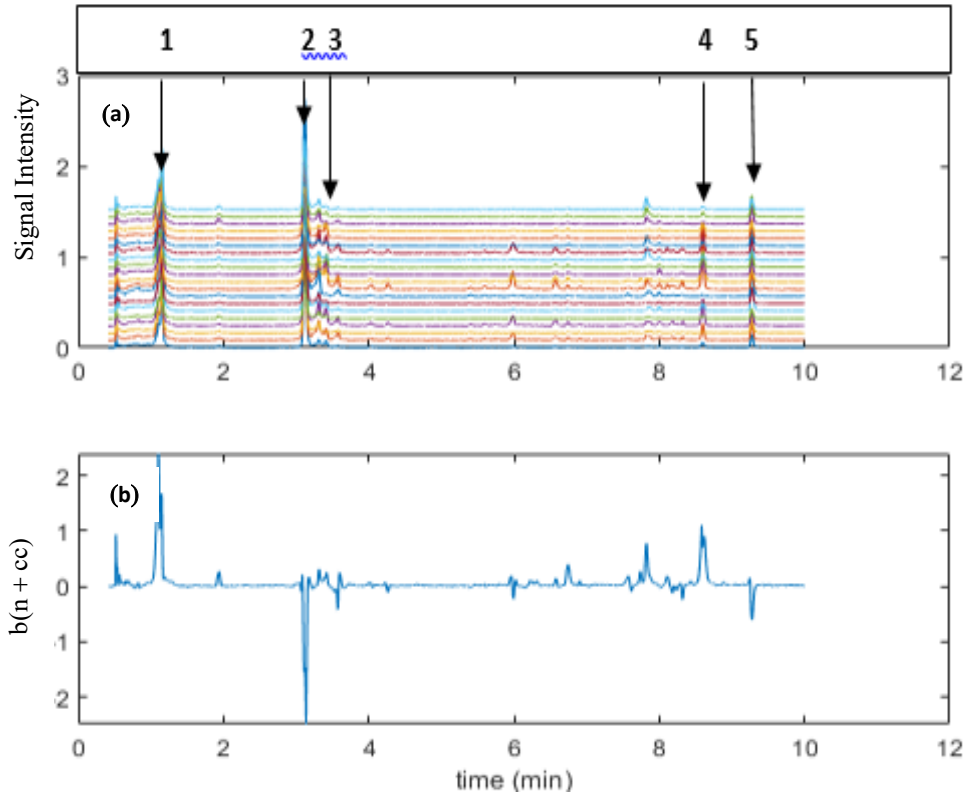

Fig.5

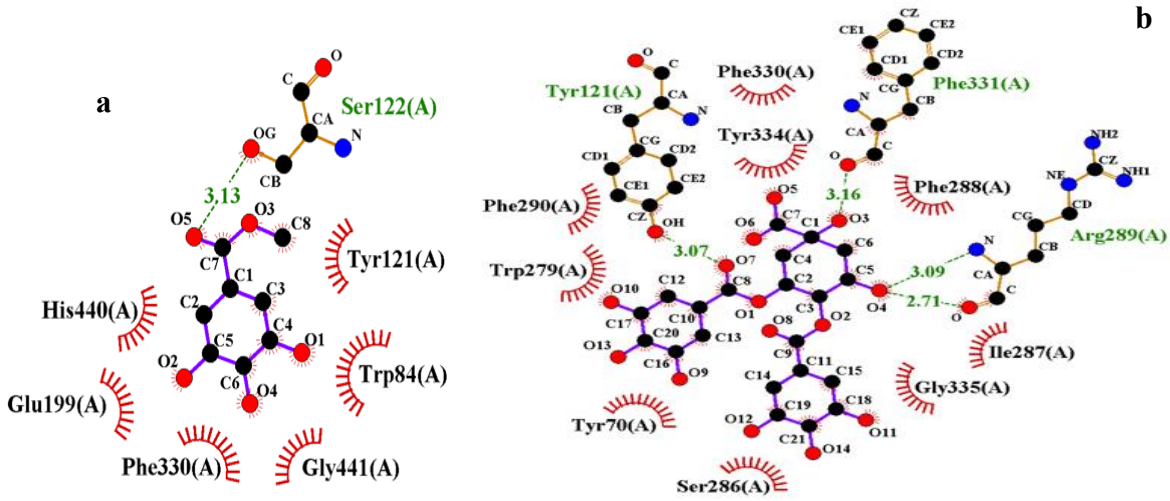
a
Ser122(A)
3.13
Tyr121(A)
His440(A)
Trp84(A)
Glu199(A)
Phe330(A)
Gly441(A)
b
Tyr121(A)
Phe330(A)
Phe331(A)
Tyr334(A)
Phe290(A)
Phe288(A)
Arg289(A)
3.16
3.07
3.09
2.71
Trp279(A)
Ile287(A)
Gly335(A)
Tyr70(A)
Ser286(A)

Fig.6

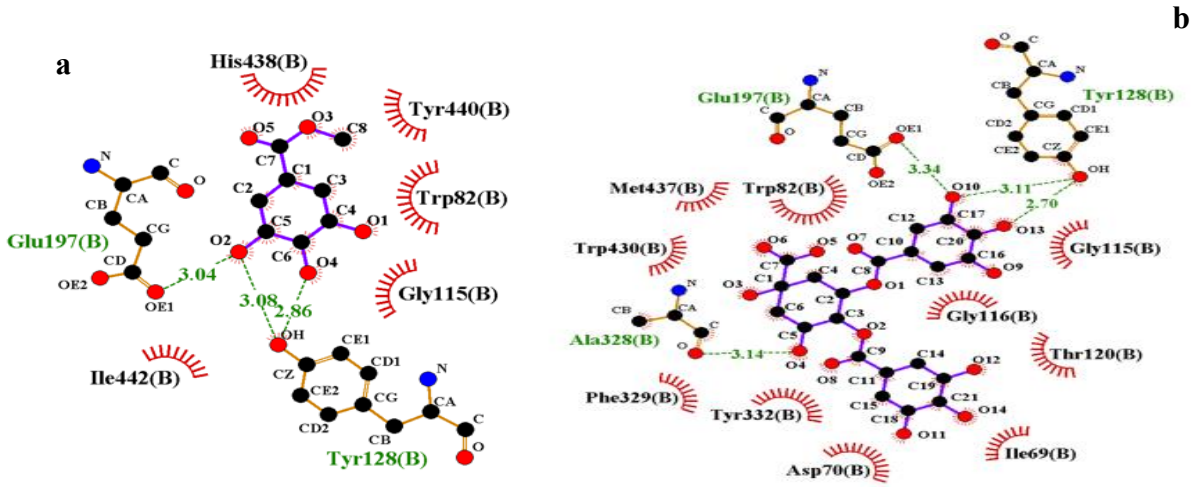
a
His438(B)
Tyr440(B)
Trp82(B)
Gly115(B)
Glu197(B)
Ile442(B)
Tyr128(B)
3.04
3.08
2.86
b
Glu197(B)
Tyr128(B)
Met437(B)
Trp82(B)
Trp430(B)
Gly115(B)
Gly116(B)
Ala328(B)
Thr120(B)
Phe329(B)
Tyr332(B)
Asp70(B)
Ile69(B)
3.34
3.11
2.70
3.14

Fig.7

Tables

Table 1 Monthly variation in the anti-AChE activity (expressed as IC_{50} in µg/mL) of PAG extracts from Laghouat and Ain Oussera.

Month	GML ±SD (n=3)	GFL ±SD (n=3)	GMA ±SD (n=3)	GFA ±SD (n=3)	GMA-GFA* ±SD (n=6)
July	63.43^{b}±2	64.53^{bc}±5	68.94^{c}±7	68.13^{c}±7	67.52±6
August	56.42^{a}±4	58.15^{a}±8	66.10^{ab}±12	63.24^{ab}±5	62.28±4
September	65.18^{b}±7	66.38^{c}±5	63.24^{ab}±8	67.35^{bc}±6	64.69±7
October	57.14^{a}±4	60.14^{ab}±7	61.33^{a}±5	62.30^{a}±9	65.47±5
November	62.74^{b}±5	65.81^{bc}±4	67.35^{bc}±8	66.00^{ab}±12	66.10±3

(GML-GFL): male (ML) and female (FL) gall collected in Laghouat, (GMA-GFA): male (MA) and female (FA) galls collected in Ain Oussera. Averages in one column with the same superscript do not differ significantly according to the Duncan *post hoc* tests. Superscripts a→ b→ c indicate increasing activities (decreasing IC_{50}).
*Average of results obtained for both genders.

Table 2 Monthly variation in the anti-BuChE activity (expressed as IC_{50} in µg/mL) of PAG extracts from Laghouat and Ain Oussera.

Month	GML ±SD (n=3)	GFL ±SD (n=3)	GMA ±SD (n=3)	GFA ±SD (n=3)	GML-GFL* ±SD (n=6)	GMA-GFA* ±SD (n=6)
July	85.86^{ab}±2	82.43^{a}±5	90.10±4	92.53±4	84.14^{a}±6	91.31±6
August	91.58^{b}±9	93.71^{b}±4	92.15±6	94.24±5	92.64^{b}±6	93.19±4
September	82.85^{a}±8	87.38^{ab}±7	91.71±3	93.52±3	85.11^{a}±6	92.61±7
October	84.14^{b}±6	83.47^{ab}±3	94.14±5	92.80±4	83.80^{a}±6	93.47±5
November	90.54^{ab}±5	95.81^{b}±8	93.52±9	92.54±4	93.11^{b}±6	92.84±3

(GML-GFL): male (ML) and female (FL) gall collected in Laghouat, (GMA-GFA): male (MA) and female (FA) galls collected in Ain Oussera. Averages in one column with the same superscript do not differ significantly according to the Duncan *post hoc* tests. Superscripts a→ b→ c indicate increasing activities (decreasing IC_{50}).
*Average of results obtained for both genders.

Table 3. Binding affinity and molecular interactions of methyl gallate and digalloylquinic acid with AChE

Ligands	Docking score(kcal/mol)	Type of interaction	Number of interactions	Residues	Distance (Å)
Methyl gallate	−6.47	Hydrogen Bond	1	Ser122	3.13
		Hydrophobic	6	Trp84 Tyr121 Glu199 Phe330 His440 Gly441	
Digalloylquinic acid	−8.26	Hydrogen Bond	4	Tyr121 Arg289 (2) Phe331	3.07 3.09/2.71 3.16
		Hydrophobic	9	Tyr70 Trp279 Ser286 Ile287 Phe288 Phe290 Phe330 Tyr334 Gly335	

Table 4. Binding affinity and molecular interactions of methyl gallate and digalloylquinic acid with BuChE

Ligands	Docking score (kcal/mol)	Type of interaction	Number of interactions	Residues	Distance (Å)
Methyl gallate	−5.98	Hydrogen Bond	3	Tyr128 (2) Glu197	3.08/2.86 3.04
		Hydrophobic	5	Trp82 Gly115 His438 Tyr440 Ile442	
Digalloylquinic acid	−9.1	Hydrogen Bond	4	Tyr128 (2) Glu197 Ala328	3.11/2.70 3.34 3.14
		Hydrophobic	10	Ile69 Asp70 Trp82 Gly115 Gly116 Thr120 Phe329 Tyr332 Trp430 Met437	

Table S1 Number of model components (#) and RMSECV of the models for enzyme inhibition, built with the fingerprints and using three preprocessing approaches.

Inhibition activity	**Preproccessing**	#	$RMSECV_{IC50}$
AChE			
	Column centering	2	18.22
	Normalization and column centering	5	23.67
	SNV and column centering	4	21.4
BuChE			
	Column centering	2	27.42
	Normalization and column centering	3	26.16
	SNV and column centering	3	28.68